Study on on-line failure detection method of lithium-ion battery based on Mie scattering theory*

LI Wen, LÜ Binbin, XU Minggang, and HAO Sijia**

Institute of Mechanical and Electrical Engineering, North China University of Technology, Beijing 100144, China

(Received 31 March 2022; Revised 26 April 2022)

Lithium-ion battery has attracted more and more attention under the background of energy crisis and environmental pollution, and safety issues have become the focus of attention. A new detection method is proposed in this paper to overcome the problems of poor versatility, low accuracy and poor sensitivity in aerosol and smoke detection in the early warning of lithium-ion battery failure. It is a photodetector based on Mie scattering theory, which can assist temperature, voltage and current data to realize online detection. The experiments have shown that a lithium-ion battery with a battery capacity of only 300 mA was overcharged under low power conditions. The aerosol and smoke generated by the battery failure and rupture were easily detected by the detector. A small amount of aerosol and smoke could be detected under overdischarge conditions, and the feasibility of the method was fully verified. The results show that on-line detection of lithium-ion battery failure can be achieved under extreme conditions with few nuisance alarms, and it is characterized by low cost, high speed, high efficiency and good universality.

Document code: A **Article ID:** 1673-1905(2022)08-0502-6

DOI https://doi.org/10.1007/s11801-022-2050-5

The lithium-ion batteries are widely used in new energy vehicles and energy storage devices because of their high operating voltage, low memory effect, and high energy density[1-3]. The failure phenomenon of lithium-ion batteries occurs in the process of production, transportation, and use, because reactive and flammable materials are inside them. The safety incidents of lithium-ion batteries have been reported over the past few years, and thus safety issues are concerned. The mechanical abuse, electrical abuse and thermal abuse are the main reasons for the thermal runaway of lithium-ion batteries. A large number of gases, aerosols and smog are generated by the thermal runaway of lithium-ion batteries accompanied by temperature increasing. The failure parameter characteristics corresponding to the various failure modes of lithium-ion batteries are very different. The failure parameter characteristics corresponding to various types of batteries with the same failure form are also different. Therefore, the gas generated by the failure of lithium-ion batteries has been extensively studied by scholars. FREDRIK et al[4] have studied the gas explosion and thermal runaway during external heating of commercial lithium-ion graphite-lithium cobalt oxide batteries with different aging degrees, and the toxic carbon monoxide, hydrogen fluoride and phosphorus oxyfluoride were detected by measuring gas emissions via Fourier transform infrared spectroscopy. FERNANDES et al[5] have used gas chromatography combined with mass spectrometry and Fourier transform infrared spectroscopy to identify and quantify the gases emitted from commercial lithium-ion batteries under the condition of overcharging. KIM et al[6] have studied the failure status of thermally abused lithium-ion batteries, and the microscopic damage of thermal abuse was monitored in situ by electrochemical impedance spectroscopy and acoustic emission techniques. BEN et al[7] have reviewed the research progress on gas evolution and its mechanism in lithium-ion batteries, and a technique for detecting and quantifying gas evolution in ex situ and in situ studies was established, which is gas chromatography-mass spectrometry and differential/on-line electrochemical mass spectrometry. WANG et al[8] have sorted out thermal runaway phenomena and related fire dynamics in single lithium cells and battery packs, potential fire protection measures were discussed, and some ideas for future development of lithium battery fire safety research and safety engineering were proposed. The above studies have found that gas, aerosol and smog are generated in the early stage of thermal runaway of lithium-ion batteries. The accuracy and sensitivity of traditional gas detectors and smoke detectors may not be able to detect the generated gases, aerosols and smoke, and are prone to false alarms.

* This work has been supported by the National Natural Science Foundation of China (No.51205005), and the Beijing Science and Technology Innovation Service Ability Building (No.PXM2017-014212-000013).

** E-mail: 1587805485@qq.com

The fault diagnosis and detection and early warning methods have been proposed by many researchers, but they cannot be applied in practice due to the large amount of data, the inability to achieve online detection, poor versatility, and excessive detection and analysis equipment. In this paper, the real-time online detection of aerosols and smog generated by lithium-ion batteries is proposed based on Mie scattering theory. The response speed of the optical sensor to smoldering fire is faster than that of the traditional ionization detector, and the nuisance alarm is not easy to occur. It has the characteristics of low cost, small structure, light weight, and long working time. It can choose more wavelengths, the spectral range is larger, and the requirements for the working environment are low.

The Mie scattering theory describes the strict mathematical solution of Maxwell's equation for uniform particles in uniform media that are irradiated by a plane monochromatic wave. When the light with a wavelength of λ an intensity of I_0 is incident on an isotropic spherical particle with a radius of r, the scattered light intensity at a certain point P according to the Mie scattering theory can be described as[9,10]

$$I_{\text{sca}} = I_0 g \frac{\lambda^2}{8\pi^2 r^2} gI(\theta,\phi), \tag{1}$$

$$I(\theta,\phi) = |S_1(\theta)|^2 \sin^2\phi + |S_2(\theta)|^2 \cos^2\phi, \tag{2}$$

where I_{sca} is the scattered light intensity, θ is the scattering angle, and ϕ is the polarization angle of polarized light. The two amplitude functions of $S_1(\theta)$ and $S_2(\theta)$ are as follows

$$S_1(\theta) = \sum_{n=1}^{\infty} \frac{2n+1}{n(n+1)} [a_n \pi_n + b_n \tau_n], \tag{3}$$

$$S_2(\theta) = \sum_{n=1}^{\infty} \frac{2n+1}{n(n+1)} [a_n \tau_n + b_n \pi_n], \tag{4}$$

where τ_n and π_n are Legendre polynomials and are related to the scattering angle θ, and a_n and b_n are related to Bessel functions as

$$a_n = \frac{\phi_n(a)\phi_n'(ma) - m\phi_n'(a)\phi_n(ma)}{\varepsilon_n(a)\phi_n'(ma) - m\varepsilon_n'(a)\phi_n(ma)}, \tag{5}$$

$$b_n = \frac{m\phi_n(a)\phi_n'(ma) - \phi_n'(a)\phi_n(ma)}{m\varepsilon_n(a)\phi_n'(ma) - \varepsilon_n'(a)\phi_n(ma)}, \tag{6}$$

where a is the dimensionless diameter, D is the actual diameter of the particle, m is the refractive index of the scattering particle relative to the surrounding medium, and $\phi_n(a)$ and $\varepsilon_n(a)$ are Bessel functions.

The Mie scattering theory is applicable to all mean spherical particles and is a general case of the scattering law. A photodetector dual-wavelength 470 nm blue light-emitting diode (LED) and a 850 nm infrared (IR) LED are adopted, and the particle sizes of various types of smoke, aerosols and water vapour are different according to different combinations of wavelengths in scattering measurements.

The soft-packed polymer lithium-ion battery is used in the experiment. Its positive electrode is composed of nickel-cobalt lithium manganate and current collector aluminum foil, and its negative electrode is composed of graphite and current collector copper foil. The diaphragm is made of materials such as polyethylene (PE) and polypropylene (PP). The soft-packed polymer lithium-ion batteries with rated capacities of 300/1 500 mA·h are taken as the research object, and the information is shown in Tab.1.

Tab.1 Soft-packed polymer lithium-ion battery information

Rated capacity (mA·h)	Model	Rated voltage (V)	Charging termination voltage (V)	Discharge cut-off voltage (V)	Thickness/width/total length (mm)
300	602030	3.7	4.2	2.7	6/20/31
1 500	703450	3.7	4.2	2.7	8/34/51

The schematic diagram of the experimental detection device is shown in Fig.1(a), where the charging and discharging module, the data acquisition module, the photodetector, the terminal and the sealed test box are included. The electric high-precision dual-range (ITECH) IT6872A DC power supply is used in overcharging, with a voltage range of 8—72 V, a current range of 1.5—9 A, and a high resolution of 1 mV/0.1 mA. The 50 W and 0.4 Ω metal aluminum shell resistor is used in overdischarge. The collecting temperature, voltage and current data are the main parameters of the data acquisition module. The PT100 thermal resistance is used to collect temperature and pasted on the surface of the lithium-ion battery. The Hikvision H10 series thermal imagers are used to monitor the overall temperature change of lithium batteries in the experiment. The ATORCH multimeter's voltage collecting wire is connected to the positive and negative poles at both ends of the battery, and its current collecting wire is connected in series between the direct current (DC) power supply and the battery. The sealed test chamber is made of acrylic sheet material for easy observation. The aerosols and fumes generated by the abuse of the battery are transported to the photoelectric detection module through the conduit, and then discharged. As shown in Fig.1(b), a complete photoelectric detection system (ADPD188BI) of optical dual-wavelength technology is used in the photodetector, which integrates a high-efficiency photoelectric measurement front-end, blue and IR LEDs and photodiode (PD). These devices are custom packaged, in which light must pass through the aerosol detection chamber and then directly from the

LED to the PD. Two optical detectors are included in the detector. The Photodetector 1 (PDET1) has an effective area of 0.4 mm^2, Photodetector 2 (PDET2) has an effective area of 0.8 mm^2, and a detector with an effective area of 1.2 mm^2 is combined by these two photodetectors.

Three sets of detection experiments under different abuse conditions were carried out at normal temperature. (1) Overcharge experiment. A lithium-ion battery with a rated capacity of 300 mA was selected. The initial state of the battery was 100% state-of-charge (SOC), and the voltage was 4.2 V. The IT6872A power supply was used at both ends of the lithium-ion battery for constant current and voltage charging. The set voltage was 6 V, the current was 6 A, and the PT100 thermal resistance was pasted on the surface of the lithium-ion battery. (2) Overdischarge experiment. A lithium-ion battery with a rated capacity of 300 mA was selected, the initial state of the battery was 100% SOC, and the voltage was 4.2 V. A 50 W and 0.4 Ω metal aluminum case resistor was used for the discharge load, and the PT100 thermal resistance was pasted on the surface of the lithium-ion battery. (3) Mechanical puncture experiment. A lithium-ion battery with a rated capacity of 1 500 mA was selected, and the initial state of the battery was 100% SOC. A steel cone with a diameter of 5 mm was used to exert force on the surface of the lithium-ion battery, and the loading was stopped when the steel cone penetrated one-third of the thickness of the battery, and the steel cone was withdrawn. The PT100 thermal resistance was pasted on the surface of the lithium-ion battery.

The overcharging is the most common failure form of lithium-ion battery systems. In the lithium-ion battery pack system module, the overcharge of a single cell fails if the charging current is not cut off in time, and the fire, explosion, and catastrophic consequences of battery packs are due to their system being damaged in overcharging. As shown in Fig.2, the response curve of the blue light source is a photoelectric signal, and the response

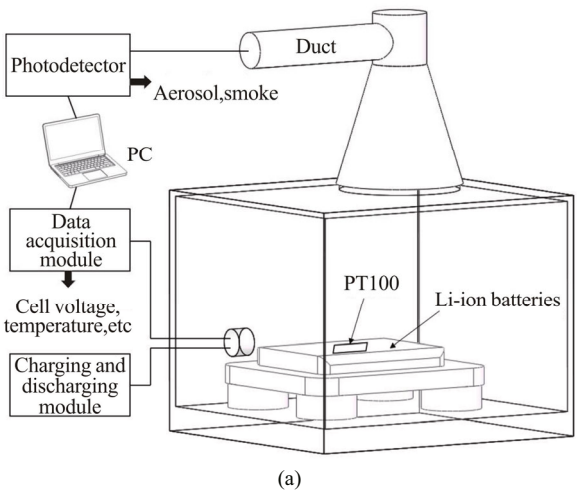

(a)

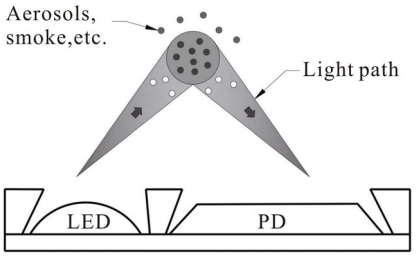

(b)

Fig.1 Schematic diagrams of experimental scheme: (a) Experimental setup; (b) Photodetector principle

is expressed as the power transfer ratio (*PTR*). It is the optical power (in nW) returned to the PD divided by the optical power (in mW) emitted by the LED.

As shown in Fig.2(a), data such as voltage, current, temperature, and photoelectric signals of lithium-ion batteries are collected during overcharge. The initial *PTR* of the photoelectric signal is 120 nW/mW. Fig.3 shows the thermal images of the lithium battery during the overcharge process, and its emissivity is denoted by ε. Fig.3(a) is the initial state of the lithium battery before overcharging, and the lithium battery starts to heat up gradually for 30 s after the start of overcharging as shown in Fig.3(b). When the overcharge is in the period of 0—100 s, the metal lithium is precipitated from the cathode and accumulated in the anode. The battery voltage gradually increases with the increase of metal lithium accumulated in the anode. The temperature of the outer surface of the battery is lower, a small amount of gas is generated, the voltage is increased from the initial 4.2 V to 4.8 V, and the battery is slightly expanded relative to the initial state of charge. In the period of 100—400 s, the voltage gradually increases from 4.8 V to 5.3 V, and almost all the cathode metal is precipitated. The battery temperature increases because the cathode resistance increases and the battery impedance also increases accordingly. The electrolyte is decomposed, and the battery has shown obvious expansion at this stage. It can be seen from the thermal image in Fig.3(c) that the battery has been deformed. The voltage and current are in a relatively stable state during the period of 400—550 s. The metal lithium is precipitated in the negative electrode and undergoes an exothermic reaction with the electrolyte, so the battery temperature rises rapidly, and the internal temperature is higher than 60 °C, the reaction is accelerated, and a large amount of gas is released. The outer layer of the aluminum foil of the battery is ruptured when the internal pressure of the battery increases for about 500 s. The photodetector detects that the gas is ejected. As shown in Fig.2(a), the photoelectric signal response curve indicates that the signal begins to rise and fluctuate sharply. It can be seen from Fig.3(d) that a small amount of gas begins to be discharged from the lithium battery. The battery temperature rises to the decomposition temperature of the PE separator (The measured battery surface temperature was about 110 °C).

Within a period of 500—650 s, the battery current and temperature drop rapidly. It can be seen from Fig.3(e) that a large amount of gas and smoke is discharged, and the photoelectric signal begins to fluctuate violently. As shown in Fig.2, the *PTR* peak reaches 142 nW/mW. After 650 s, the failure of the battery disconnects the external loading power supply, the current gradually drops to 0, the voltage is reduced to 4.2 V and remains unchanged, and the photoelectric signal is also restored to its original value with the removal of gas and smoke, as shown in Fig.3(f).

The different types of smoke and common sources of interference are distinguished by means of dual wavelengths, and the photodetector's ability to exclude sources of interference and avoid false alarms is improved. The changes in particle size of aerosols and smoke emitted from lithium batteries can be seen by the ratio of blue light response to infrared response over time, and no false alarms are generated. As shown in Fig.2(b), the gases, aerosols, and smoke begin to be detected by photodetectors, and the ratio curve rises rapidly, peaking at 0.98.

The overdischarge can cause irreversible capacity loss to the battery. As shown in Fig.4(a), the initial value of the photodetector *PTR* is 121 nW/mW. Within 30 s after the lithium-ion battery is powered on, the two processes of delithiation of the negative electrode and lithiation of the positive electrode are carried out simultaneously during the continuous discharge process of the lithium-ion battery. The voltage drops sharply from 3 V to 1.6 V, the current drops from 3.5 A to 2 A, and the temperature is basically stable at this stage. The temperature starts to rise 30 s after the battery is powered on, the dissolution reaction of the copper current collector begins, the negative electrode voltage is brought into the plateau phase of the electrochemical reaction, and the copper ions of the solvent can enter the electrolyte, pass through the separator and deposit to the positive electrode. The decomposition of the solid electrolyte interphase film and the generation of gas are due to the excessive delithiation of the negative electrode, and the voltage and current start to decrease slowly after 60 s of increase. The formation of internal shorts is due to the increased deposition of copper ions, and the temperature reaches a maximum at 480 s. At the same time, the aluminum foil of the battery ruptured and the gas released are detected by the photodetector because the internal pressure of the battery gradually increases, and then the temperature begins to drop, and the voltage and current gradually decrease to 0. The formation of holes in the porous negative electrode, the collapse of the electrode material structure and the saturation of the positive electrode material are due to the continuous movement of lithium ions in the lithiated negative electrode to the positive electrode during the overdischarge process.

The overcharge and overdischarge are both the electric abuse of lithium battery failure. The failure mode is roughly the same from the surface observation, which is the slow expansion of the battery. The gases and fumes are released because the internal pressure ruptures as shown in Fig.4, and the discharge releases much less gas and smoke than overdischarge. The interfering signal appears in the 570—590 s time period. It is inferred that some of the gas or smoke is released because of the transient disturbance caused by the inclusion of liquid particles, which is barely visible to the naked eye.

The research believes that the puncture test is a method of simulating a short circuit in the battery. The experimental mechanism is that the battery undergoes chemical and electrochemical reactions in a short time under extreme conditions of use, and the internal short circuit of the battery is because the internal structure of the battery changes, a lot of heat and smoke gas is released, and the battery is caught on fire and exploded.

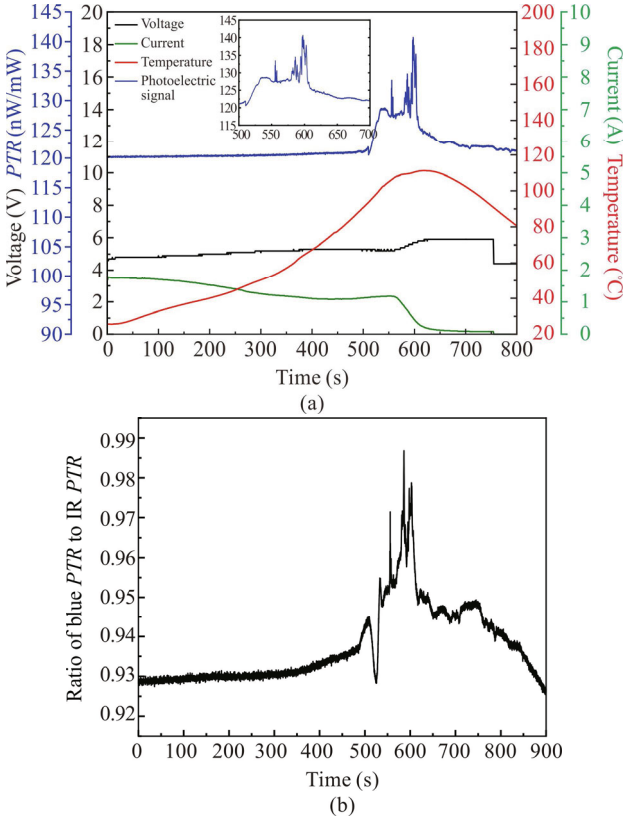

Fig.2 Experimental data of overcharge: (a) Real-time detection data of overcharge; (b) Ratio of blue *PTR* to IR *PTR*

The steel needle with a diameter of 5 mm was used experimentally to rapidly pierce the middle of a fully charged single cell with a capacity of 100% SOC. When the puncture needle passes through the battery, a large amount of gas and smoke is released from the damaged small hole at 87 s. The photoelectric signal rises sharply, and the battery temperature has reached 60 °C. The signal is stable for about 30 s at the peak of 350 nW/mW, due to a large amount of gas and smoke cannot be expelled in time. The signal rises briefly because the battery discharge is discontinuous at 138 s. The battery surface

temperature reaches 120 °C within 3 min, and there is no fire. The ratio of blue light to infrared response is shown in Fig.5(b). The 1 500 mA lithium battery is used for puncturing, and the smoke released has high concentration, large particle size and short duration compared to the 300 mA battery used for charging and discharging.

The feasibility of photodetectors for failure detection of lithium batteries under extreme working conditions was verified by three sets of experiments, overdischarge, overcharge and puncture. The experimental results show that the detection of aerosols and smoke generated when lithium batteries fail can be realized by photodetectors based on Mie scattering theory. And the on-line monitoring of auxiliary current, voltage and temperature and other data information was realized, batteries with smaller capacity were selected, and various tests were carried out. Therefore, the method has high development and application value. The performance and reliability of the entire battery pack is affected by the failure of a single lithium cell, and the battery pack stops working or other safety issues are created, and the development and research of "sensing-structure-sensing" integrated smart battery is provided through this method. Secondly, new energy vehicles, electric vehicles, energy storage power stations, portable electronic devices and other fields can be applied. The above research shows that this method has the characteristics of low cost, rapidity, high efficiency and good versatility, and on-line detection, low

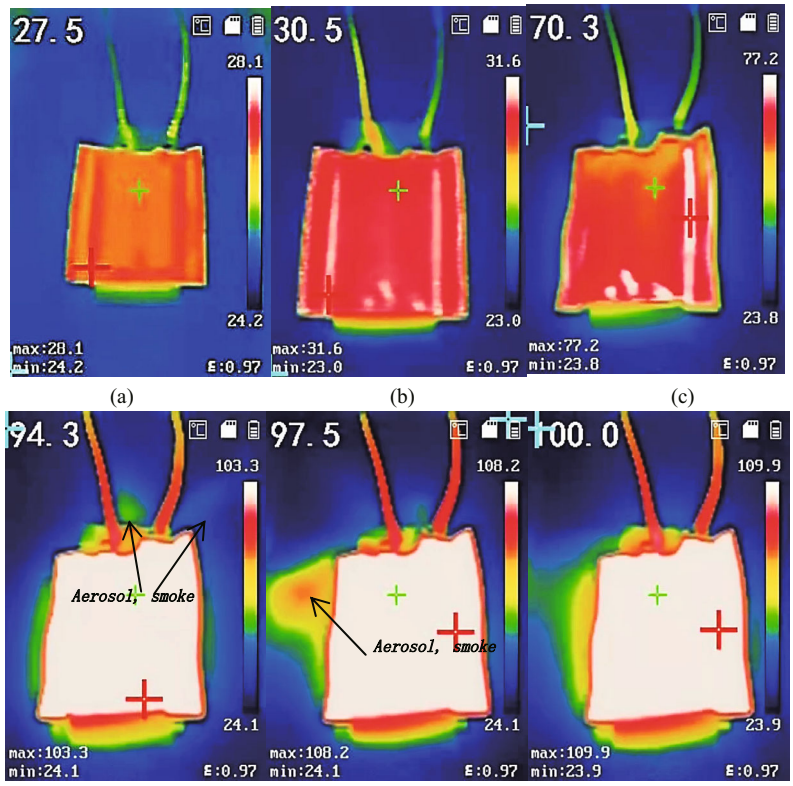

Fig.3 Thermal images of lithium battery during overcharge: (a) 0 s; (b) 30 s; (c) 400 s; (d) 500 s; (e) 550 s; (f) 650 s

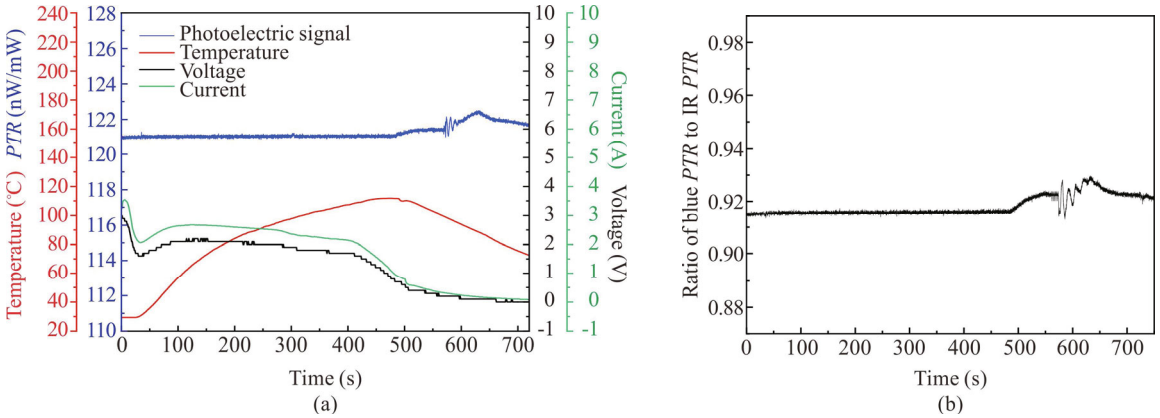

Fig.4 Experimental data of overdischarge: (a) Real-time detection data of overdischarge; (b) Ratio of blue *PTR* to IR *PTR*

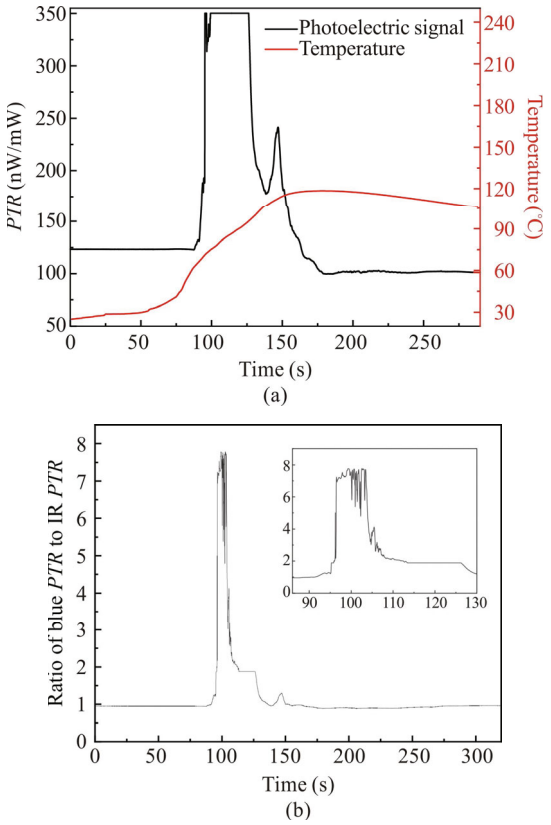

Fig.5 Experimental data of puncture: (a) Real-time detection data of puncture; (b) Ratio of blue *PTR* to IR *PTR*

power consumption, reducing false positives from other sources of interference in harsh environments can be achieved.

Statements and Declarations

The authors declare that there are no conflicts of interest related to this article.

References

[1] CHEN M Y, OUYANG D X, LIU J, et al. Investigation on thermal and fire propagation behaviors of multiple lithium-ion batteries within the package[J]. Applied thermal engineering, 2019, 157：113750.

[2] WANG X B, WU F T, YAO M H. A life-prediction method for lithium-ion batteries based on a fusion model and an attention mechanism[J]. Optoelectronics letters, 2020, 16(6)：410-417.

[3] ZHANG C, GUO Y, WANG C, et al. A new design of experiment method for model parametrisation of lithium ion battery[J]. Journal of energy storage, 2022, 50：104301.

[4] FREDRIK L, SIMON B, MAURIZIO F, et al. Gas explosions and thermal runaways during external heating abuse of commercial lithium-ion graphite-$LiCoO_2$ cells at different levels of ageing[J]. Journal of power sources, 2018, 373：220-231.

[5] FERNANDES Y, BRY A, PERSIS S. Identification and quantification of gases emitted during abuse tests by overcharge of a commercial Li-ion battery[J]. Journal of power sources, 2018, 389：106-119.

[6] KIM J Y, WANG Z L, LEE S M, et al. Failure analysis of thermally abused lithium-ion battery cell by microscopy, electrochemical impedance spectroscopy, and acoustic emission[J]. Microelectronics reliability, 2019, 100-101：113363.

[7] BEN R, NURIA G A. A review of gas evolution in lithium ion batteries[J]. Energy reports, 2020, 6(Supl.5)：10-18.

[8] WANG Q S, MAO B B, STANISLAV I, et al. A review of lithium-ion battery failure mechanisms and fire prevention strategies[J]. Progress in energy and combustion science, 2019, 73：95-131.

[9] MANUEL N V. Fundamentals of Mie scattering[M]// Woodhead publishing series in electronic and optical materials. Cambridge：Woodhead Publishing, 2014, 202：39-72.

[10] ZHANG H, NIE W, LIANG Y, et al. Development and performance detection of higher precision optical sensor for coal dust concentration measurement based on Mie scattering theory[J]. Optics and lasers in engineering, 2021, 144：106642.